Advanced ECG Signal Classification for Early Arrhythmia Detection Using Deep Learning and Comparative Algorithms

Naveen Kumar Penjerla
School of Electronics Engineering, VIT-AP University, Amaravathi, Andhra Pradesh, India
naveen.penjerla@gmail.com

Sudha Ellison Mathe
School of Electronics Engineering, VIT-AP University, Amaravathi, Andhra Pradesh, India
ellison.mathe@vitap.ac.in (corresponding author)

Received: 13 January 2026 | Revised: 24 February 2026, 2 April 2026, and 10 April 2026 | Accepted: 17 April 2026

 DOI: https://doi.org/10.48084/etasr.17512

ABSTRACT

This study proposes a robust framework that combines contour-based feature extraction with Deep Neural Networks (DNNs) for reliable arrhythmia detection. The approach was evaluated on the MIT-BIH arrhythmia database, where preprocessing techniques, such as wavelet transform, empirical mode decomposition, and adaptive digital filtering, were applied to suppress baseline wander, power line interference, muscle artifacts, and electrode noise. Comparative experiments were conducted using Support Vector Machines (SVMs) and k-Nearest Neighbors (KNNs) classifiers. The results demonstrated that while SVM achieved an accuracy of 97% and KNN reached 73.9%, the proposed DNN model outperformed both, with a classification accuracy of 99.3%. These findings revealed the potential of the proposed system to enhance the accuracy and robustness of ECG-based diagnostics, offering a reliable tool for early-stage arrhythmia detection and supporting timely clinical decision-making.

Keywords-ECG; Arrhythmia; MIT-BIH; Deep Neural Network; Feature Extraction; SVM; KNN

I. INTRODUCTION

Cardiovascular diseases are one of the leading causes of mortality worldwide; thus, their accurate, early detection is significant in order to mitigate their impact. The Electrocardiogram (ECG) is the most widely utilized non-invasive tool for monitoring cardiac function and diagnosing abnormalities, such as myocardial infarction, Atrioventricular (AV) block, ventricular tachycardia, and atrial fibrillation. Reliable interpretation of ECG signals, however, is often challenged by noise interference as well as the subtle variations present in arrhythmic patterns.

Several methods have been developed to improve the accuracy of arrhythmia detection. Classical approaches, including the Pan-Tompkins algorithm and wavelet-based filtering techniques, have been extensively applied for QRS detection and noise suppression [1, 2]. While effective to a certain extent, these techniques often fail to reconstruct signals consistently and lose important morphological details when subjected to high levels of noise. In parallel, Machine Learning (ML) methods, like Support Vector Machines (SVM), and k-Nearest Neighbors (KNN) have been employed for ECG classification. These frameworks, however, rely heavily on hand-crafted features and demonstrate limited adaptability to complex and large-scale datasets.

Advances in Deep Learning (DL) have exhibited significant capability for biomedical signal analysis. Convolutional and recurrent neural networks, in particular, have achieved strong performance in ECG classification tasks by automatically extracting high-level features [3]. Yet, challenges remain in achieving robust detection in noisy environments and ensuring real-time applicability.

To address these challenges, the current study introduces a Deep Neural Network (DNN) architecture combined with contour-based feature extraction for accurate arrhythmia classification [4-6]. Unlike conventional approaches, the current method leverages adaptive filtering and morphological operations to enhance peak detection while minimizing false classifications. The evaluation of the proposed DNN framework was achieved using the MIT-BIH arrhythmia database against SVM and KNN classifiers.

Accordingly, the recognition and classification of arrhythmias remain challenging, particularly in noisy environments and large-scale datasets. This gap motivates the development of advanced ML and DL frameworks capable of learning noise-resilient features directly from raw or minimally pre-processed signals. By integrating robust preprocessing with automated feature extraction, such systems are likely to offer higher diagnostic accuracy and reliability in both clinical and real-time monitoring applications.

II. LITERATURE REVIEW

The analysis of ECG signals has been extensively studied using a variety of signal processing and ML techniques. Previous studies have focused primarily on noise reduction and QRS detection, which form the foundation for reliable arrhythmia classification.

Authors in [7-11] applied discrete wavelet transforms to isolate frequency components for noise removal. While effective in separating low- and high-frequency bands, their reconstruction phase suffered from distortion, resulting in reduced fidelity of the restored signal. Similarly, authors in [12] explored frequency decomposition for denoising, but the reassembled signals presented corruption of original features, limiting clinical applicability.

Subsequent research sought to address these shortcomings. In [13], a frequency grouping and peak point identification method was introduced, which improved noise suppression and allowed better reconstruction. Building on this, the GQRS algorithm demonstrated improved *R*-peak detection by combining frequency grouping with morphological corrections, leading to higher accuracy in noise-affected signals. However, these approaches were constrained by their dependence on handcrafted features and fixed rules.

Discrete wavelet transform-based denoising has been extensively explored for ECG preprocessing [14]; however, reconstruction artifacts often distort morphological fidelity [15]. A comparative review of selected approaches is summarized in Table I, highlighting algorithms, feature extraction strategies, and performance outcomes.

TABLE I. A REVIEW OF VARIOUS ALGORITHMS FOR CLASSIFICATION OF ECG ARRHYTHMIA

Ref. No	Methodology	Key Features/techniques	Reported accuracy	Remarks
[5]	1D CNN with channel-wise attention	Multi-spatial deep feature extraction, Multi-channel P-QRS-T wave segmentation, Baseline wander suppression	> 99%	High accuracy; strong detection of ectopic beats via dynamic attention; patient-specific approach requiring local calibration
[6]	Siamese Convolutional Neural Network (SCNN)	Few-shot similarity learning paradigm, Dual twin convolutional tracking, Pairs-wise similarity and loss profiling, 12-lead imbalanced data optimization	Up to 95% (hold-out) 89% mean AUC (7-fold)	Bypasses large data reliance; highly robust at detecting rare anomalies with few training samples; outscores traditional architectures on multi-lead diagnostic structures
[16]	GLCM-enhanced Convolutional Neural Network	3D multi-scale GLCM generation, Texture-based shape feature extraction, Automated statistical feature mapping, Morphological footprint tracking	92.14%	Efficient in extracting subtle wave features; reduces misdiagnosed computerized interpretations; performance is slightly lower than attention-based deep models
[17]	Multi-Modal Hybrid Deep Learning	Multi-modal data fusion (CT, MRI, ECG), 3D-UNet for 3D imaging features, Temporal Conv Graph Net (TC-GNN), Heterogeneous feature fusion layer	97.1%	Successfully overcomes single-modality structural bottlenecks found in basic CNN/LSTM models; delivers highly comprehensive risk profiling by merging electrical and structural telemetry

These studies represent a move toward multi-modal, noise-resilient, and interpretable ECG systems capable of edge deployment, confirming that effective preprocessing integrated with efficient DL architectures is essential for reliable and scalable arrhythmia classification in contemporary biomedical applications. The literature highlights a clear evolution:

- Signal processing methods improved noise suppression but failed to preserve morphological fidelity.
- Classical ML advanced classification, but required extensive optimization in feature extraction and training. Classical ML classifiers, such as SVM and KNN, demonstrate reasonable accuracy when combined with handcrafted features, but their generalization capability is limited in noisy or large-scale datasets [18, 19].
- DL models achieved high accuracy, yet their sensitivity to noise and reconstruction errors remains a barrier for real-world deployment. DL models, including CNNs, RNNs, and attention-based architectures [20, 21], have achieved state-of-the-art performance in ECG classification by automatically learning hierarchical features [22].

Heart disease prediction frameworks incorporate multi-modal medical data, including clinical attributes, imaging, and physiological signals, to enhance diagnostic robustness and support comprehensive cardiovascular risk assessment. Thus, there is a lack of continuity between preprocessing (noise suppression) and classification (feature learning) in most existing works. Limited frameworks simultaneously optimize for noise robustness, morphological preservation, and classification accuracy.

III. DATASET AND METHODOLOGY

The proposed framework was developed to address the challenges identified in previous ECG arrhythmia detection approaches. Traditional signal processing methods improved noise suppression but frequently distort ECG morphology, while classical ML methods depend heavily on handcrafted features and often fail to generalize across noisy conditions.

To overcome these limitations, the current study introduces a framework that integrates morphological preprocessing, contour-based feature extraction, and a DNN for accurate arrhythmia classification. The complete workflow is illustrated in Figure 1.

The proposed methodology is structured into three main stages:

- ECG signal preprocessing and noise suppression
- Contour-based feature extraction and *R*-peak optimization
- Classification using ML and DL models

The system was developed and validated using the MIT-BIH Arrhythmia Database [23, 24], which contains 48 half-hour two-channel ECG recordings sampled at 360 Hz. Each ECG record was segmented into 10-s windows to standardize training samples. The resulting dataset consisted of approximately 150 segments, including both normal and arrhythmic beats. The class distribution was 35% normal and 65% arrhythmic. All data are annotated by expert cardiologists. Table II presents the characteristics of the MIT-BIH dataset.

To prevent data leakage and ensure reliable evaluation, an inter-patient data partitioning strategy was adopted, where ECG segments from the same patient were not shared between the training and testing sets. The dataset was divided into 70% training, 15% validation, and 15% testing, with an additional 5-fold cross-validation applied.

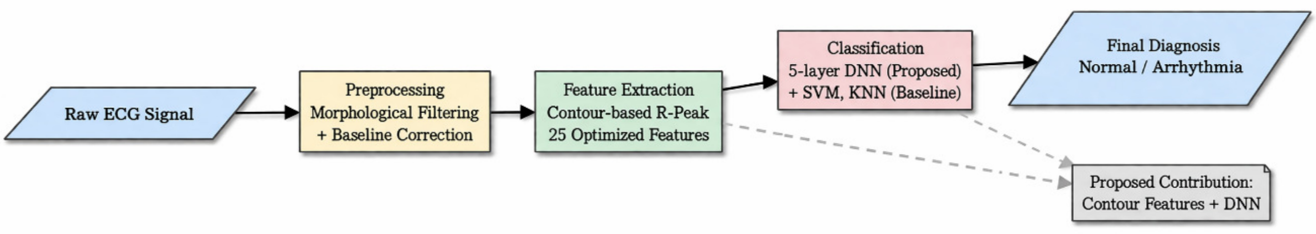

Fig. 1. Flow chart for proposed methodology.

TABLE II. CHARACTERISTICS OF THE MIT-BIH ARRHYTHMIA DATABASE

Property	Description
No. of records	48 half-hour two-channel ECG recordings
Sampling frequency	360 Hz per channel, 11-bit resolution
Lead configuration	Modified Lead II and one precordial lead [25]
Duration	~30 min per record
Annotation	Labelled by cardiologists (normal, supraventricular, ventricular, fusion, paced beats) [26]
Noise inclusion	Baseline wander, power line interference, muscle noise, electrode artifacts

A. *ECG Signal Preprocessing*

ECG recordings from the MIT-BIH arrhythmia database contain several forms of noise, including baseline wander, muscle activity, electrode motion artifacts, and power line interference. These disturbances can significantly reduce the accuracy of R-peak detection and arrhythmia classification [27, 28]. Therefore, an effective preprocessing stage is essential to preserve ECG morphology while suppressing unwanted artifacts.

1) *Morphological Filtering*

To enhance signal quality, a morphological filtering approach was applied to raw ECG data. This stage involves two complementary operations:

- Dilation: This operation expands the waveform amplitudes. While it emphasizes dominant structures, it is not used in isolation for *R*-peak detection as it may exaggerate spurious noise peaks.
- Erosion: It smooths the signal by reducing small fluctuations and eliminating unwanted notches. By observing neighboring values, it suppresses additional peaks, which helps isolate the true QRS complex.

2) *Baseline Wander Removal*

After morphological filtering, baseline correction was applied to eliminate low-frequency drift. The filtered minimum values were subtracted from the original ECG signal to generate a stable baseline reference.

The baseline-corrected ECG signal is expressed as:

$$X_f = X_{min} - f_{min} \quad (1)$$

The ECG signal (X_{min}) subtracts the filtered signal (f_{min}) and obtains the baseline (X_f). This operation helps in adjusting the minimum points of the signal.

The erosion-filtered ECG signal is represented as:

$$X_e = X - X_f \quad (2)$$

This is how a simple mathematical morphological filter works in the preprocessing stage and helps extract the best signal form and peak points with ease.

B. *Filtration*

Figure 2 presents the filtration pipeline used for noise suppression through morphological filtering and frequency decomposition. The process begins with the acquisition of the raw ECG signal, which represents the electrical activity of the heart. In practical scenarios, ECG recordings are often contaminated by different types of noise, such as baseline wander, power-line interference, and muscle artifacts. Variable Mode Decomposition (VMD) was applied as an initial step to decompose the ECG signal into several sub-signals, each corresponding to a specific frequency band. This helps in effectively separating meaningful cardiac information from noise components.

After decomposition, the extracted frequency components were analyzed and compared with standard ECG frequency ranges and commonly observed noise frequencies. Components outside the expected ECG spectrum were identified as noise and were removed.

A four-level filtering mechanism was then applied to further suppress residual noise. Intermediate outputs (Signals 2-4, Figure 2) represent filtered components obtained at different stages of the process. These signals were combined to reconstruct a cleaner ECG signal that preserves essential morphological characteristics while significantly reducing noise.

To further enhance noise suppression, an adaptive filtering scheme was incorporated into the framework. Adaptive filters automatically adjust their parameters based on the characteristics of the noise present in the signal, allowing more accurate noise estimation and cancellation. The effectiveness of this filtering process was evaluated using performance metrics that measure both noise reduction and signal preservation. The reconstructed ECG signal obtained at this stage was suitable for further clinical analysis, such as arrhythmia detection and other diagnostic evaluations.

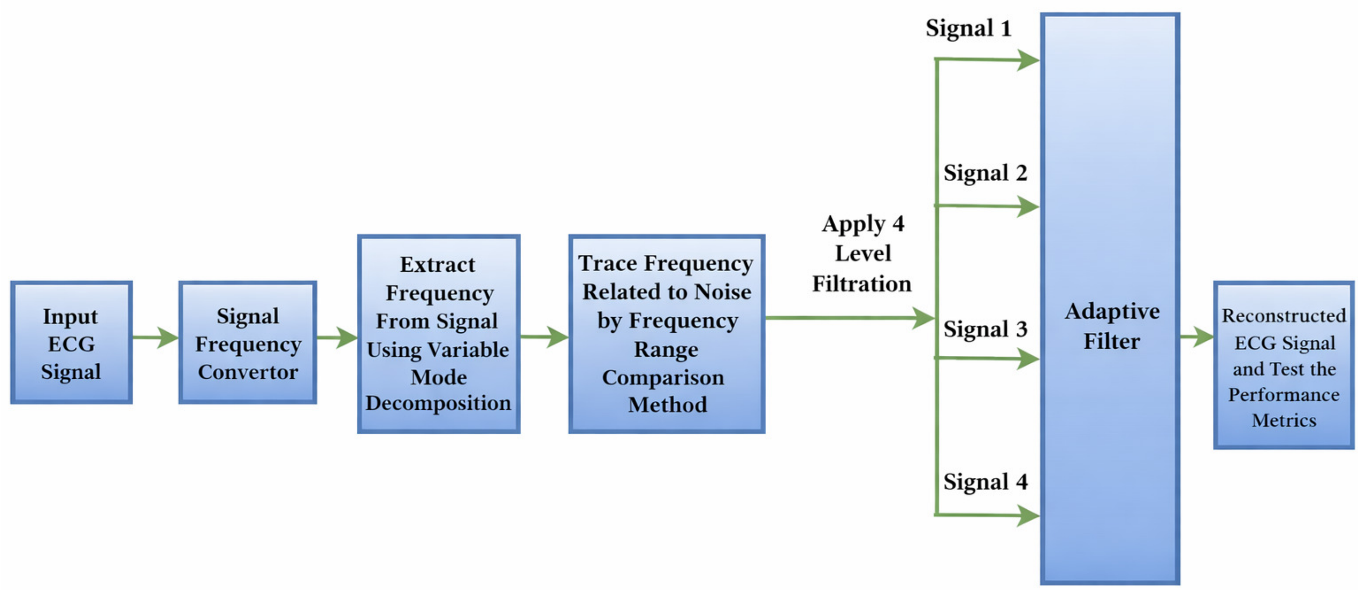

Fig. 2. Block diagram to extract the noise.

C. *Contour-Based Feature Extraction*

Unlike traditional morphological feature extraction methods that rely on fixed QRS interval measurements, the proposed contour-based feature extraction strategy employed adaptive amplitude thresholds and dual-stage correction filtering. This enables robust *R*-peak identification under noisy conditions while reducing false detections.

The feature extraction stage consists of two major steps.

1) *Peak Candidate Detection*

Maximum and minimum contour points were identified for each 10-s segment. Weak peaks, determined by a threshold relative to the segment's highest amplitude, were discarded.

2) *Peak Correction and Optimization*

False positives were eliminated by cross-checking candidate peaks against QRS morphology, yielding a refined set of 25 representative feature points per sample.

This method ensured that extracted features retain clinically relevant information while minimizing the effect of noise.

D. *Classification Models*

Three classifiers were evaluated in this study: SVM, KNN, and the proposed DNN.

1) *Support Vector Machine (SVM)*

Performs well on small, linearly separable datasets but struggles with nonlinearities in noisy signals.

2) *k-Nearest Neighbors*

The KNN is a simple distance-based classifier, highly sensitive to noise, and less efficient for large datasets.

3) *Proposed Deep Neural Network*

Designed as a five-layer sequential model with the following structure:

- Input layer: 25 contour features
- Three hidden layers: progressively reducing dimensions (25 →12 → 8)
- Output layer: binary classification (normal versus arrhythmia)

Figure 3 illustrates the architecture of the proposed framework. The hidden layers utilize the Rectified Linear Unit (ReLU) activation function to learn complex and non-linear relationships while avoiding issues such as vanishing gradients. The output layer uses a sigmoid activation function to generate a probability value that indicates whether a given ECG segment contains noise or not.

The ReLU activation is defined as:

$$f(x) = \begin{cases} 0 & \text{for } x < 0 \\ x & \text{for } x > 0 \end{cases} \quad (3)$$

To minimize this error rate, an error cost function (C) needs to be applied on the network by considering inputs and biasing conditions, while the error rate will be updated on every portion of the signal.

Let us consider the input from (2) and compute this through a linear function to obtain the output:

$$y = Xe \quad (4)$$

Then the C is computed concerning the input variables:

$$C(w,b) = \frac{1}{2n}\sum_x \|y(X_e) - a\|^2 \quad (5)$$

The DNN was trained using forward propagation and backpropagation. During training, the prediction error was calculated using a binary cross-entropy loss function, and the model parameters were updated through optimization techniques, such as stochastic gradient descent or Adam. After training, the model could classify new ECG segments by comparing the predicted probability with a fixed threshold. This approach enables reliable identification of noisy ECG signals and improves the overall accuracy of ECG analysis in practical applications.

Two regularizing parameters were considered for the learning rate (η) and the vectorizing tuning parameter (σ). As per the standard function, the intermediary values were considered:

$$\omega_k \to \omega'_k = \omega_k - \eta \frac{\partial C}{\partial w_k} \quad (6.1)$$

$$b_l \to b'_b = b_l - \eta \frac{\partial C}{\partial b_l} \quad (6.2)$$

The cost function updating in intermediatory/intermediary values is given by:

$$\nabla C = \frac{1}{n}\sum_x \nabla C_x \quad (7)$$

As the training portion commences, the X_e is a set of $\{X_{e1}, X_{e2}, X_{e3}, \dots, X_{em}\}$, and the intermediatory/intermediary value is updated by:

$$\frac{\sum_{j=1}^{m} \nabla C_{xj}}{m} = \frac{\sum_x \nabla C_x}{n} = \nabla C \quad (8)$$

Then, (6.1) and (6.2) are updated with training values:

$$\omega_k \to \omega'_k = \omega_k - \frac{\eta}{m}\sum_{j=1} \frac{\partial C}{\partial w_k} \quad (9.1)$$

$$b_l \to b'_b = b_l - \frac{\eta}{m}\sum_{j=1} \frac{\partial C}{\partial b_l} \quad (9.2)$$

From these, the activation function (a) for the updating of weights with the j^{th} layer function was defined as:

$$a_j^l = \sigma\left(\sum_k w_{jk}^l a_k^{l-1} + b_j^l\right) \quad (10)$$

From (9.1) and (9.2), (10) was reconfigured to:

$$a^l = \sigma(w^l a^{l-1} + b^l) \quad (11)$$

The error rate was optimized by the parameter:

$$\delta_l^j = \sum_k w_{jk}^l \delta_k^{l-1} \odot \sigma_j^l \quad (12)$$

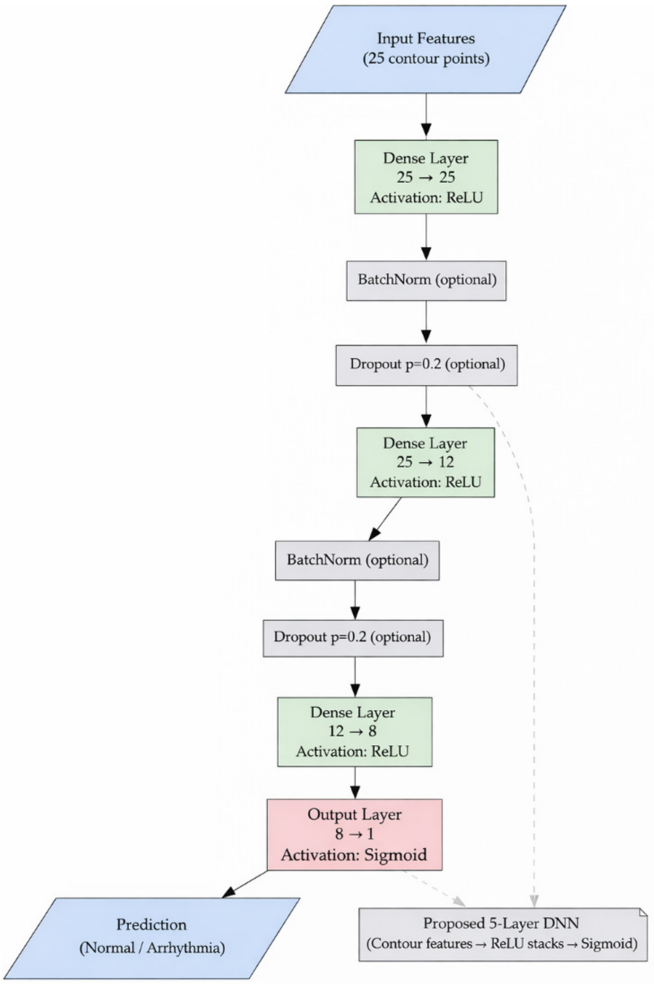

Fig. 3. Architecture of DNN.

Equation (12) was updated by the ReLU function to optimize the weights of DNNs with a combination of two layers. The first was compiled with 25 feature intakes and optimized to 12 points, while the next phase provided an 8-stage outcome. In the final stage, the sigmoid function acted to optimize/optimized the error rate in linear mode and extended the effective results to the prediction outcome.

The proposed five-layer DNN architecture leverages the strengths of ReLU and sigmoid activation functions to effectively recognize and classify noise in ECG signals. The methodology involves preprocessing, feature extraction, DNN processing, training, and classification, each contributing to the network's ability to minimize error rates and improve the accuracy of its predictions. By enhancing the reliability of ECG diagnostics, this approach ultimately contributes to better patient outcomes and more precise clinical decision-making.

IV. RESULTS

All classifiers were tested using the same separate acquired dataset and similar contour-based features. An inter-patient split was utilized, where no subjects seen in testing were used in training. The evaluation was conducted on the test set in terms of accuracy, sensitivity, specificity, precision, F1-score, and ROC-AUC. In addition to these, a 5-fold cross-validation was performed, reporting the mean across folds.

All models were optimized using grid search. Specifically,

- KNN: $k \in \{3, 5, 7, 9\}$; best performance achieved at $k = 5$ using Euclidean distance.
- SVM: Kernel: Radial Basis Function (RBF) $C \in \{0.1, 1, 10\}$ Gamma $\in \{0.01, 0.001\}$. Best configuration: C = 10, gamma = 0.01.
- Proposed DNN: Layers: 25 → 12 → 8 → 1, Activation: ReLU (hidden), Sigmoid (output), Optimizer: Adam (*lr* = 0.001), Epochs: 100 (early stopping), Batch size: 32.

The proposed contour-based algorithm successfully identified *R*-peaks across different records in the MIT-BIH dataset. Contour-based morphological features provide a compact and physiologically meaningful representation of ECG waveforms, improving robustness against noise [29]. On average, 25 optimized features per 10-s segment were extracted after discarding spurious peaks and correcting false detections. The resulting contours, after correction, matched the annotated *R*-peaks fairly well, which indicated that the method was robust in noisy environments. This stage ensured that only those features that are physiologically meaningful passed to the classifiers, thus minimizing error propagation. The architecture of the proposed DNN is based on good design practices for ECG classification, where ReLU is used for the feature learning layer and sigmoid for the binary classification layer [30].

The experimental setup was designed to ensure reproducibility and fair evaluation of the proposed framework. The system configuration, software tools, dataset partitioning, and training parameters are presented in Table III. The hardware and software environment ensured that the training and evaluation of the DNN could be performed efficiently. The dataset was split into training, validation, and test sets to avoid overfitting as well as to provide an unbiased estimate of generalization performance. The utilization of 5-fold cross-validation further strengthened the robustness of the evaluation.

TABLE III. EXPERIMENTAL SETUP

Category	Specification
Hardware	Intel Core i7 (10th Gen @ 2.9 GHz), 16 GB RAM, NVIDIA GTX 1660 Ti (6 GB), Windows 11 Pro
Software	Python 3.13, TensorFlow 2.12, Keras, NumPy, SciPy, scikit-learn, Matplotlib, Py Wavelets
Dataset partition	70% training, 15% validation, 15% testing, 5-fold cross-validation
Training parameters	Optimizer: Adam (*lr* = 0.001), Batch size: 32, Epochs: 100 (with early stopping), Loss: Binary Cross-Entropy
Regularizatio n	Dropout (*p* = 0.2), Batch Normalization
Activation	ReLU (hidden layers), Sigmoid (output layer)
Evaluation metrics	Accuracy, Sensitivity (Recall), Specificity, Precision, F1-score, ROC-AUC

Model training incorporated an adaptive learning rate through the Adam optimizer, alongside dropout and batch normalization to maintain robust regularization. The metrics used for measuring performance included accuracy, sensitivity, specificity, precision, F1 score, and ROC-AUC, all of which were computed across both properly and improperly balanced classes.

To mathematically assess classification behavior, Sensitivity and Specificity were defined as:

- Sensitivity is the proportion of events (true positives) correctly classified:

$$\text{Sensitivity} = \frac{TP}{TP + FN}$$

- Specificity is the proportion of true negatives correctly identified among all actual negatives:

$$\text{Specificity} = \frac{TN}{TN + FP}$$

A comparative analysis of isolated feature extraction strategies is presented in Table IV, demonstrating that contour-based features provide improved accuracy.

TABLE IV. FEATURE EXTRACTION-BASED CLASSIFICATION

Feature extractor	Sample size	TP	TN	FP	FN	Sensitivity	Specificity	Accuracy
Wavelet feature extractor	51 data points (10sec)	28	10	12	1	0.965517	0.909	0.745
Hermite transform coefficients	51 data points (10sec)	27	10	12	2	0.931034	0.833	0.725
ST + WT + Temporal	51 data points (10sec)	34	10	4	3	0.918919	0.76	0.862
Contour features	51 data points (10sec)	39	8	4	0	0.909	0.72	0.93

Table V presents some comparative results in performance across combinations of traditional ML and DL methodologies. The results confirm that the proposed contour feature extraction, when combined with the DNN model, exhibited the highest classification accuracy (0.987) along with the lowest computational latency (0.48 s).

Figure 4 illustrates the performance metrics (sensitivity, specificity, and accuracy), calculated for ECG data samples extracted from the MIT-BIH database, on different feature extractors. Among these algorithms, the proposed method exhibited the optimum accuracy, effective sensitivity, and specificity from the *R*-Peak detection stages. Figure 5 depicts the percentages of accuracy of different classifiers under the contour feature process.

TABLE V. FEATURE EXTRACTION AND CLASSIFICATION COMBINATIONS

Feature extractor	Sample size	Time (s)	Accuracy
Wavelet feature extractor + BGRU [22]	51 data points (10 s)	2.00	0.9855
DWT based [14]	51 data points (10 s)	1.00	0.960
Contour features (proposed) + SVM	51 data points (10 s)	0.98	0.96
Contour features (proposed) + KNN	51 data points (10 s)	1.40	0.795
Contour features (proposed) + DNN	51 data points (10 s)	0.48	0.987

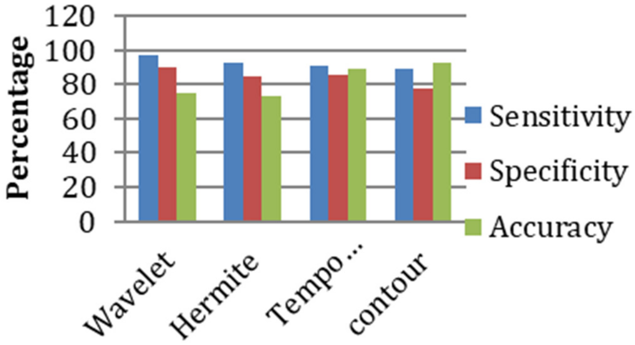

Fig. 4. Performance metrics on different features extracted.

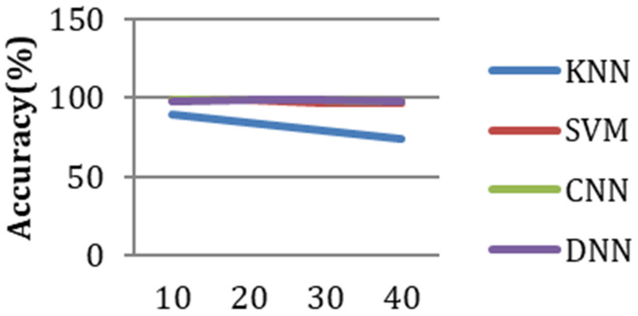

Fig. 5. Accuracy of different classifiers tested under the contour feature process.

While SVM offers decent performance, it lacks in computational efficiency and overall accuracy. Its delay in processing each sample makes it less suitable for real-time applications where quick decision-making is crucial. On the other hand, DNN provides a significant improvement in accuracy and processing speed compared to SVM. It balances precision and recall well, making it a reliable choice for ECG noise classification. However, it still has the possibility for improvement in computational efficiency. The DNN model excels in all evaluated metrics, making it the best choice among the three. Its high accuracy and low computational delay demonstrate its capability to effectively handle the complexities of ECG signal classification. The model's ability to extract relevant features through convolutional layers contributes to its high effectiveness in distinguishing noise from clean signals.

TABLE VI. SUMMARY OF PERFORMANCE METRICS

Classifier	Accuracy (%)	Sensitivity (%)	Specificity (%)	Precision (%)	F1-score (%)	AUC
KNN	73.9	71.5	75.8	70.2	70.8	0.78
SVM	97.0	96.4	97.6	96.8	96.6	0.97
CNN	98.82	97.56	97.89	97.63	98.4	0.98
DNN (proposed)	99.3	99.1	99.5	99.2	99.1	0.99

Table VI presents the final performance metrics across classifiers. The findings revealed that an AUC of 0.78 was achieved with KNN, reflecting weak discriminative ability. The curve is closer to the diagonal, indicating frequent misclassifications in distinguishing between normal and arrhythmic beats. An AUC of 0.97 was calculated with SVM, suggesting strong performance with high sensitivity and specificity. However, the curve indicated slight degradation in noisy conditions, consistent with the model's reliance on manually crafted features. The proposed methodology reached an AUC of 0.99, with the ROC curve lying closest to the top-left corner. This demonstrates near-perfect classification and robustness against both false positives and false negatives.

The performance of the classifiers was further evaluated using the ROC and AUC curves. Figure 6 displays the ROC curves of KNN, SVM, and the proposed DNN classifier. The ROC-AUC results confirm that the proposed DNN not only achieves superior accuracy but also provides consistent performance across different decision thresholds.

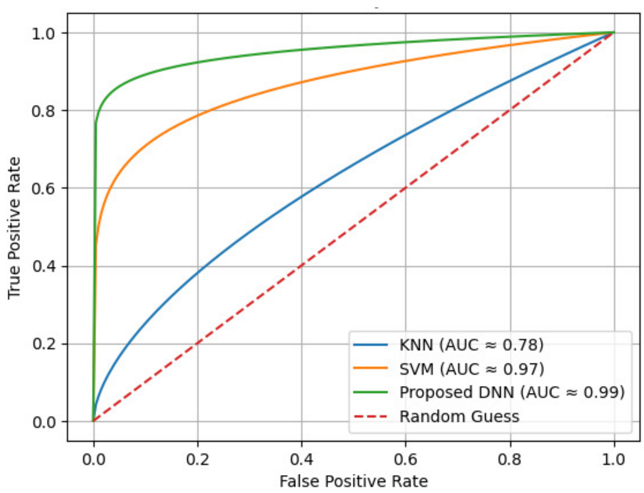

Fig. 6. ROC-AUC analysis curve.

This is critical in clinical practice, where the cost of a false negative (missed arrhythmia) is higher than that of a false positive. The near-perfect AUC of 0.99 highlights the DNN's potential for reliable real-time arrhythmia detection.

V. CONCLUSION

This study introduced a Deep Neural Network (DNN) framework combined with contour-based feature extraction for reliable arrhythmia detection. The approach was evaluated on the MIT-BIH arrhythmia database, where preprocessing techniques, such as wavelet transform, empirical mode decomposition, and adaptive digital filtering, were applied to suppress baseline wander, power line interference, muscle artifacts, and electrode noise. The method was subjected to inter-patient cross-validation as well as all-inclusive comparative studies with the state-of-the-art, validating the performance and computational efficiency for real-time applications. The results delivered 99.3% accuracy, with 99.1% sensitivity, 99.5% specificity, and AUC ≈ 0.99 on MIT-BIH, outperforming SVM (97.0% accuracy; AUC ≈ 0.97) and KNN (73.9% accuracy; AUC ≈ 0.78). These findings indicate strong discrimination across thresholds and robustness to common ECG noise.

However, there are several limitations: the evaluation centered on a single two-lead benchmark with fixed sampling (360 Hz), so generalization to multi-lead clinical ECGs, alternative devices, and real-world ambulatory settings was unproven; runtime and energy profiles on wearables/edge hardware were not profiled; and the current implementation focused on binary detection rather than full multi-class rhythm taxonomy or rare arrhythmias.

Future work will focus on:

- Broadening validation to multi-lead, multi-cohort datasets and cross-database testing
- Extending to multi-class classification with calibrated probabilities, cost-sensitive loss, and class-imbalance strategies
- Pursuing deployment-oriented optimization quantization/pruning and low-latency inference with target budgets (e.g., <10 ms per 10 s window, <50 mW average power on embedded SoCs)
- Integrating patient-specific adaptation mechanisms and drift detection algorithms for home monitoring
- Reporting full clinical metrics, including per-class F1, PPV/NPV, and time-to-alarm statistics, alongside ablations quantifying the contribution of preprocessing and contour features

These steps move the system from benchmark success toward reliable, real-time clinical use.

DECLARATION OF COMPETING INTERESTS

The authors declare that they have no known competing financial interests or personal relationships that could have appeared to influence the work reported in this paper.

ACKNOWLEDGMENT

Not applicable to this work.

DATA AVAILABILITY

The dataset used in this research are available in [23, 24].

REFERENCES

[1] A. E. M. Atwa, E.-S. Atlam, A. Ahmed, M. A. Atwa, E. M. Abdelrahim, and A. I. Siam, "Interpretable Deep Learning Models for Arrhythmia Classification Based on ECG Signals Using PTB-X Dataset," *Diagnostics*, vol. 15, no. 15, Aug. 2025, Art. no. 1950, https://doi.org/10.3390/diagnostics15151950.

[2] A. Shaheen, L. Ye, C. Karunaratne, and T. Seppänen, "Fully-Gated Denoising Auto-Encoder for Artifact Reduction in ECG Signals," *Sensors*, vol. 25, no. 3, Jan. 2025, Art. no. 801¸https://doi.org/10.3390/s25030801.

[3] S. Sattar *et al.*, "Cardiac Arrhythmia Classification Using Advanced Deep Learning Techniques on Digitized ECG Datasets," *Sensors*, vol. 24, no. 8, Apr. 2024, Art. no. 2484, https://doi.org/10.3390/s24082484.

[4] K. Hanbay, "Deep neural network based approach for ECG classification using hybrid differential features and active learning," *IET Signal Processing*, vol. 13, no. 2, pp. 165–175, 2019, https://doi.org/10.1049/iet-spr.2018.5103.

[5] F. Li, J. Wu, M. Jia, Z. Chen, and Y. Pu, "Automated Heartbeat Classification Exploiting Convolutional Neural Network With Channel-Wise Attention," *IEEE Access*, vol. 7, pp. 122955–122963, Aug. 2019, https://doi.org/10.1109/ACCESS.2019.2938617.

[6] M. M. Eduardo Vasconcellos *et al.*, "Siamese Convolutional Neural Network for Heartbeat Classification Using Limited 12-Lead ECG Datasets," *IEEE Access*, vol. 11, pp. 5365–5376, Jan. 2023, https://doi.org/10.1109/ACCESS.2023.3236189.

[7] U. Satija, B. Ramkumar, and M. S. Manikandan, "A New Automated Signal Quality-Aware ECG Beat Classification Method for Unsupervised ECG Diagnosis Environments," *IEEE Sensors Journal*, vol. 19, no. 1, pp. 277–286, Jan. 2019, https://doi.org/10.1109/JSEN.2018.2877055.

[8] U. Satija, B. Ramkumar, and M. S. Manikandan, "Automated ECG Noise Detection and Classification System for Unsupervised Healthcare Monitoring," *IEEE Journal of Biomedical and Health Informatics*, vol. 22, no. 3, pp. 722–732, May 2018, https://doi.org/10.1109/JBHI.2017.2686436.

[9] J. Huang, B. Chen, B. Yao, and W. He, "ECG Arrhythmia Classification Using STFT-Based Spectrogram and Convolutional Neural Network," *IEEE Access*, vol. 7, pp. 92871–92880, July 2019, https://doi.org/10.1109/ACCESS.2019.2928017.

[10] S. S. Xu, M.-W. Mak, and C.-C. Cheung, "Towards End-to-End ECG Classification With Raw Signal Extraction and Deep Neural Networks," *IEEE Journal of Biomedical and Health Informatics*, vol. 23, no. 4, pp. 1574–1584, July 2019, https://doi.org/10.1109/JBHI.2018.2871510.

[11] N. Feng, S. Xu, Y. Liang, and K. Liu, "A Probabilistic Process Neural Network and Its Application in ECG Classification," *IEEE Access*, vol. 7, pp. 50431–50439, Apr. 2019, https://doi.org/10.1109/ACCESS.2019.2910880.

[12] H. Ma and L. Xia, "Atrial Fibrillation Detection Algorithm Based on Graph Convolution Network," *IEEE Access*, vol. 11, pp. 67191–67200, June 2023, https://doi.org/10.1109/ACCESS.2023.3291352.

[13] X. Zhai and C. Tin, "Automated ECG Classification Using Dual Heartbeat Coupling Based on Convolutional Neural Network," *IEEE Access*, vol. 6, pp. 27465–27472, May 2018, https://doi.org/10.1109/ACCESS.2018.2833841.

[14] C. Venkatesan, P. Karthigaikumar, A. Paul, S. Satheeskumaran, and R. Kumar, "ECG Signal Preprocessing and SVM Classifier-Based Abnormality Detection in Remote Healthcare Applications," *IEEE Access*, vol. 6, pp. 9767–9773, Jan. 2018, https://doi.org/10.1109/ACCESS.2018.2794346.

[15] J. Mao, Z. Li, S. Li, and J. Li, "A Novel ECG Signal Denoising Algorithm Based on Sparrow Search Algorithm for Optimal Variational

Modal Decomposition," *Entropy*, vol. 25, no. 5, May 2023, Art. no. 775, https://doi.org/10.3390/e25050775.

[16] W. Sun, N. Zeng, and Y. He, "Morphological Arrhythmia Automated Diagnosis Method Using Gray-Level Co-Occurrence Matrix Enhanced Convolutional Neural Network," *IEEE Access*, vol. 7, pp. 67123–67129, May 2019, https://doi.org/10.1109/ACCESS.2019.2918361.

[17] P. Archana and S. V. Shashikala, "A Hybrid Deep Learning Heart Disease Prediction Framework Utilizing Multi-Modal Medical Imaging and Novel Feature Fusion Techniques," *Engineering, Technology & Applied Science Research*, vol. 15, no. 6, pp. 28596–28602, Dec. 2025, https://doi.org/10.48084/etasr.13204.

[18] X. An, S. Shi, Q. Wang, Y. Yu, and Q. Liu, "Research on a Lightweight Arrhythmia Classification Model Based on Knowledge Distillation for Wearable Single-Lead ECG Monitoring Systems," *Sensors*, vol. 24, no. 24, Dec. 2024, Art. no. 7896, https://doi.org/10.3390/s24247896.

[19] B.-T. Pham, P. T. Le, T.-C. Tai, Y.-C. Hsu, Y.-H. Li, and J.-C. Wang, "Electrocardiogram Heartbeat Classification for Arrhythmias and Myocardial Infarction," *Sensors*, vol. 23, no. 6, Mar. 2023, Art. no. 2993, https://doi.org/10.3390/s23062993.

[20] S. Ikram *et al.*, "Transformer-based ECG classification for early detection of cardiac arrhythmias," *Frontiers in Medicine*, vol. 12, Aug. 2025, https://doi.org/10.3389/fmed.2025.1600855.

[21] M. Lee, J. Lim, and J. Kim, "ECG-GraphNet: Advanced arrhythmia classification based on graph convolutional networks," *Heart Rhythm O2*, vol. 6, no. 8, pp. 1199–1211, Aug. 2025, https://doi.org/10.1016/j.hroo.2025.05.012.

[22] H. M. Lynn, S. B. Pan, and P. Kim, "A Deep Bidirectional GRU Network Model for Biometric Electrocardiogram Classification Based on Recurrent Neural Networks," *IEEE Access*, vol. 7, pp. 145395–145405, Sept. 2019, https://doi.org/10.1109/ACCESS.2019.2939947.

[23] G. B. Moody and R. G. Mark, "The impact of the MIT-BIH Arrhythmia Database," *IEEE Engineering in Medicine and Biology Magazine*, vol. 20, no. 3, pp. 45–50, June 2001, https://doi.org/10.1109/51.932724.

[24] G. B. Moody and R. G. Mark, "MIT-BIH Arrhythmia Database." PhysioNet, 1992, https://doi.org/10.13026/C2F305.

[25] H. Wang, T. Shen, S. Jiang, J. Wang, Y. Ma, and Y. Zhang, "Visualized Lead Selection for Arrhythmia Classification Based on a Lead Activation Heatmap Using Multi-Lead ECGs," *Bioengineering*, vol. 11, no. 6, June 2024, Art. no. 578, https://doi.org/10.3390/bioengineering11060578.

[26] M. Scarpiniti, "Arrhythmia Detection by Data Fusion of ECG Scalograms and Phasograms," *Sensors*, vol. 24, no. 24, Dec. 2024, Art. no. 8043, https://doi.org/10.3390/s24248043.

[27] A. E. Curtin, K. V. Burns, A. J. Bank, and T. I. Netoff, "QRS Complex Detection and Measurement Algorithms for Multichannel ECGs in Cardiac Resynchronization Therapy Patients," *IEEE Journal of Translational Engineering in Health and Medicine*, vol. 6, pp. 1–11, June 2018, https://doi.org/10.1109/JTEHM.2018.2844195.

[28] R. A. Félix, A. Ochoa-Brust, W. Mata-López, R. Martínez-Peláez, L. J. Mena, and L. L. Valdez-Velázquez, "Fast Parabolic Fitting: An R-Peak Detection Algorithm for Wearable ECG Devices," *Sensors*, vol. 23, no. 21, Oct. 2023, Art. no. 8796, https://doi.org/10.3390/s23218796.

[29] W. Zhu, X. Chen, Y. Wang, and L. Wang, "Arrhythmia Recognition and Classification Using ECG Morphology and Segment Feature Analysis," *IEEE/ACM Transactions on Computational Biology and Bioinformatics*, vol. 16, no. 1, pp. 131–138, Jan. 2019, https://doi.org/10.1109/TCBB.2018.2846611.

[30] Q. Xiao *et al.*, "Deep Learning-Based ECG Arrhythmia Classification: A Systematic Review," *Applied Sciences*, vol. 13, no. 8, Apr. 2023, Art. no. 4964, https://doi.org/10.3390/app13084964.